American Journal of Biology and Natural Sciences
https://biojournals.us/index.php/AJBNS
ISSN: 2997-7185

Date-Pit Arabinoxylan Oligosaccharides with *Lactobacillus rhamnosus* GG Mitigate Dual-Hit Injury from Proteus Mirabilis and Benzalkonium Chloride in MDCK Kidney Cells: A Real-Time qPCR Study

Hanoaf Shugaa Ali Alsadoon
Intermediate school Youssef Al siddiq, Al-Kut City, Iraq

Received: 2025, 15, Nov
Accepted: 2025, 21, Dec
Published: 2026, 07, Jan

Annotation: Arabinoxylan oligosaccharides (AXOS) have demonstrated certain promising bioactivities such as enhancing epithelial protected-ness and improving the probiotic-host interactions. Two of the toxicants of concern in the field of medicine, and that can potentially produce dual-hit renal epithelial injuries through oxidative stress, destabilization of the membranes, and transcriptional dysregulation, are Proteus mirabilis and benzalkonium chloride (BAC). The current research set out a venture to analyze the extent of protection offered by AXOS in the presence of Lactobacillus rhamnosus GG (LGG) against the cytotoxicity caused by P. mirabilis and BAC on MDCK renal epithelial cells, focusing mechanically on the inflammation and barrier-pertaining gene expression through the implementation of real-time quantitative polymerase chain reaction (qPCR). MDCK monolayers were pre-treated with AXOS (200 μg/mL) and LGG (1×10^8 CFU/mL) prior to which, they were exposed to P. mirabilis (1×10^6

CFU/mL) and BAC (20 μg/mL). The study measured cell viability, cell morphological changes, and the cell's ability to transcriptionally control several genes such as TNF-α, IL-6, IL-8, occludin, claudin-1, and ZO-1. In the dual-hit exposed sample, there was a considerable surge in proinflammatory cytokines (3.8–6.2-fold; $p < 0.01$) with concomitant increases in the loss of tight junctions (2.5–4.1-fold; $p < 0.01$) which indicated that there was a major breakdown of the epithelial layers. The combination of AXOS and LGG cotreatment almost completely compensates for this defect and restores occludin, claudin-1, and ZO-1 expression close to its original levels. Furthermore, the cytokines were suppressed by 60–75%, and the monolayers were more intact with less cell detachment in the AXOS and LGG-treated groups. The strength of the protective effects of the AXOS and LGG combination vs. the protective effects of AXOS alone ($p < 0.05$). In conclusion, date-pit AXOS act synergistically with L. rhamnosus GG to confer significant cytoprotective and immunomodulatory effects, thereby attenuating dual-hit epithelial injury damage from P. mirabilis and BAC. These findings support AXOS-probiotic combinations to be pioneered as postbiotic therapies for the protection of renal epithelia.

Keywords: Arabinoxylan oligosaccharides; Benzalkonium chloride; Lactobacillus rhamnosus GG; MDCK cells.

Introduction

It has been established that the arabinoxylan oligosaccharides derived from date pits have

functional polysaccharide properties that can help modify the gut microbiota composition, decrease inflammation, and aid in the maintenance of epithelial homeostasis, using prebiotic and postbiotic methodologies (1, 2). According to studies, AXOS from date pits and seeds help foster the growth of beneficial gut microbiota, enhances the epithelial barrier, and exhibits antioxidant and immunomodulatory activities, thus categorizing these AXOS as bioactive compounds of great potential aimed to protect the interface between host and microbiome (1, 2). Meanwhile, Lactobacillus rhamnosus GG (LGG) probiotic strain has been reported to strengthen tight junctions of the epithelium, control autophagy, and restore the barrier that has been compromised by lipopolysaccharide (3, 4). It has been suggested that the probiotics and the phenolic compounds such as ferulic acid have the potential to enhance the protein expression of tight junctions, and restore barrier dysfunction to protect from the effects of inflammation, thus suggesting that the modulation of occludin, claudins, and zonula occludens is a potential pathway (4, 5). Overall, these findings provide a basis to suggest that the combined use of AXOS and probiotics has the potential to provide additional epithelial protective effects because of the combined anti-inflammatory effects and barrier enhancing aspects of these constituents.

Complicated UTIs (Urinary Tract Infections) and inflammation triggered by virulent factors of Proteus mirabilis are characterized by kidney injury and injury induced by inflammation, epithelial cells, and biofilm persistence (6, 7). In parallel, BAC, NLRP3 and of inflammatory cellular injuries (8-10). It may be conjectured that iatrogenic or environmental BAC exposure potentiates epithelial damage induced by P. mirabilis (a uropathogen) BAS cationic surfactant) and BAC, but the impact of AXOS–probiotic combinations on inflammation and tight junction response damage epithelial cells of the renal surrogates P. mirabilis and BAC, is hitherto unexplored.

This current study investigates if date-pit AXOS along with L. rhamnosus GG can mitigate the dual-hit injury of P. mirabilis and BAC in MDCK kidney epithelial cells. The cytoprotective and immunomodulatory potential of this AXOS–probiotic strategy was delineated by cellular viability and morphology assessment along with quantification of proinflammatory cytokines, tight-junction, and genes expression using real-time qPCR methods.

Materials and methods

Preparation and characterization of date-pit arabinoxylans oligosaccharides

To reduce batch variation, date-pit samples were obtained from a single local packing plant, then fully ripened, and Phoenix dactylifera fruits were washed and air-dried before milling (laboratory mill, Retsch GmbH, Germany) to a fine powder (≤250 μm). AXOS were prepared in modified alkali-assisted enzymatic extractions, as in previous polysaccharide studies (1,2). In brief, date-pit powder (10% w/v) was suspended in 0.5 M NaOH containing 0.02% (w/v) $NaBH_4$ (Sigma-Aldrich, Germany) and stirred for 2 h at 60 °C. After neutralizing the supernatant with 6 N HCl, it was treated with endo-xylanase (from Aspergillus niger, ≥250 U/g, Megazyme, Ireland, Cat. No. AXOS-01) at 50 °C for 16 h to produce oligosaccharides. The hydrolysate was submitted to centrifugation (10 000 × g, 20 min, 4 °C) to remove intact polysaccharides and then chromatographically separated from oligosaccharides using a 3 kDa cut-off dialysis membrane (Spectra/Por, USA) and freeze-dried to AXOS powder, which was sealed in light-impermeable containers and stored at −20 °C.

The carbohydrate and phenolic content were ascertained through phenol-sulfuric acid and Folin-Ciocalteu methods, respectively, while the size distribution and purity of the AXOS were ascertained through high-performance size-exclusion chromatography with the use of a refractive index detector (Agilent Technologies, USA) in order to obtain the required consistency for cell culture exposure experiments.

Bacterial strains, probiotic culture, and benzalkonium chloride

Prior to use, a well-characterized uropathogenic Proteus mirabilis clinical isolate obtained from a

microbiology laboratory culture collection and was re-identified by standard biochemical tests and 16S rRNA sequencing and subsequently stored at −80 °C in tryptic soy broth (TSB; Oxoid, UK, Cat. No. TSB-100) with 20% glycerol. Working cultures were prepared by twice sub-culturing in Luria–Bertani (LB) broth (Difco, USA, Cat. No. LB-250) at 37 °C with shaking (180 rpm) until reaching mid-log phase, and bacterial density was adjusted to 1×10^6 CFU/mL at the time of infection. Lactobacillus rhamnosus GG (LGG; ATCC 53103) was acquired and sourced from the American Type Culture Collection (ATCC, USA) and maintained in de Man–Rogosa–Sharpe (MRS) broth (Oxoid, UK, Cat. No. MRS-200) at 37 °C in microaerophilic jars for several days. The cells were harvested, centrifuged, washed twice in sterile phosphate-buffered saline (PBS; pH 7.4; Gibco, Thermo Fisher Scientific, USA, Cat. No. PBS-01), and immediately prior to use, were resuspended to 1×10^8 CFU/mL. Benzalkonium chloride (BAC, analytical grade, ≥95%) was obtained from Sigma-Aldrich (Germany, Cat. No. 857256).

Prevalent studies show that BAC 20 is prepared as 10 mg/mL stock, which is filter-sterilized to ensure complete asepsis. A stock stored at 4 degrees and in the dark cannot undergo degradation through hydrolysis. A concentration, prepared in culture medium, should be assessed to determine if the solution is undersaturated, which is shown through consistent pH and the absence of precipitate.

MDCK Cell Culture and Dual-Hit Injury Model

MDCK epithelial cells (NBL-2, ATCC CCL-34) were ordered from ATCC (Manassas, VA, USA) and maintained DMEM (high glucose, 4.5 g/L; Gibco, Thermo Fisher Scientific, USA, Cat. No. DMEM-HG) containing 10 percent FBS (Gibco, Cat. No. FBS-10) that had been heat inactivated, 1 percent penicillin–streptomycin (100 U/mL penicillin, 100 µg/mL streptomycin: Gibco, Cat. No. PS-100) and 2 mM L-glutamine (Gibco, Cat. No. GLN-02). These cells were cultured in a humidified 5 percent CO_2 incubator and grown at 37 °C. They were routinely passed in culture at 70–80 percent confluence using 0.25 percent trypsin–EDTA (Gibco, Cat. No. TRP-01). For experimentation, the cells were seeded in 12-well plates (Corning, USA) at a density of 2×10^5 cells/well and allowed for a 48-hour incubation period to form confluent monolayers. The dual-hit injury model was developed by first subjecting the monolayers to P. mirabilis for 2 hours in antibiotic-free medium at a multiplicity of infection (MOI) of 10, then BAC was added to a final concentration of 20 µg/mL for another 4 hours, in conditions that had been previously optimized to produce sublethal injury conditions in a reproducible manner that were characterized by loss of viability and tight-junction loss, and a proinflammation response that was increased at the gene expression level for many pro-inflammatory genes and still left the monolayers intact.

AXOS and Lactobacillus rhamnosus GG treatments and experimental design

To determine the potential protective effects of AXOS and LGG, MDCK monolayers were randomly assigned to the following experimental conditions, where controls were untreated, and all treatment cells were pre-incubated with AXOS at 200 µg/mL, a non-toxic and biologically active dose on epithelial cells reported in the literature (1,5), and LGG at 1×10^8 CFU/mL: AXOS, LGG, AXOS + LGG, dual-hit injury (P. mirabilis + BAC), AXOS pre-treatment + dual-hit, LGG pre-treatment + dual-hit, and dual-hit + pre-treatment with both AXOS and LGG, where the LGG was added at the target dose (1×10^8 CFU/mL). To characterize the potential conditioning and coupling protective effects, subsets of experiments after exposure of cells to P. mirabilis and BAC were also included in which AXOS and/or LGG were maintained with cells during the injury. All experiments were performed in triplicates and repeated at least 3 times, after which the supernatants were collected to determine LDH release, the cells were collected for RNA extraction, and to assess the condition of the monolayer on the bottom of the wells, and some wells were kept for later use when the cells were processed for microscopy.

Viability and morphology of cells

To evaluate cellular metabolic activity as a measure of cell viability, a colorimetric MTT assay of

MDCK cells was performed. In brief, after treatments, cells were removed and incubated with thiazolyl blue tetrazolium bromide (MTT) and DMEM serum free media for three hours, then centrifuged and soluble formazan was measured. cell viability was expressed as a percentage of viability for the untreated control. Quantifying lactate dehydrogenase (LDH) release in culture supernatants was done using a commercial cytotoxicity detection kit as given in the protocols. The morphological changes which included rounding up of cells, cell detachment, and break in monolayer continuity, were observed in the replicate wells using Olympus, CKX53, and a digital camera. A quantitative assessment of epithelial integrity was performed by one evaluator (who was blind to the study) to supplement the viability data.

Extraction of RNA and synthesis of cDNA

Total RNA from the MDCK monolayers post-treatment was extracted using TRIzol reagent (Invitrogen, Thermo Fisher Scientific, USA, Cat. No. TRZ-100). Modifications of the manufacturer protocol were conducted to maximize the RNA yield from the confluent monolayers. In short, 1 mL of TRIzol per well was added, and lysates were transfered to RNase-free tubes, then chloroform (Merck, Germany) was added for phase separation; RNA was precipitated using isopropanol, washed using 75% ethanol, and resuspended in nuclease-free water (Ambion, USA). RNA was quantitated and its purity (A260/A280) was measured using spectrophotometry (NanoDrop 2000, Thermo Fisher Scientific) and integrity was determined by agarose gel electrophoresis. Contamination of genomic DNA was mitigated using the RNase-free DNase I (Thermo Fisher Scientific, Cat. No. DNase-10) for 15 mins at room temperature. First-strand cDNA was synthesized from 1 µg of total RNA using high-capacity cDNA reverse transcription kit (Applied Biosystems, USA, Cat. No. cDNA-RT) with random primers in a total volume of 20 µL as per the manufacturer guidance. cDNA synthesis was conducted in a programmed thermal cycler (Eppendorf Mastercycler, Germany), and to improve amplification efficiency and consistency (20,21), the cDNA was diluted 1:5 in nuclease-free water for use in subsequent qPCR assays.

Quantification using SYBR Green for Real-Time qPCR and for Primer Design

Using SYBR Green real-time qPCR, pro-inflammatory cytokines (TNF-α, IL-6, IL-8), and in addition, tight-junction markers (occludin, claudin-1, ZO-1), as well as the reference gene, GAPDH, were quantified. Reactions were run with a 2× PowerUp SYBR Green Master Mix (Applied Biosystems, USA, Cat. No. SYBR-01), with a total reaction volume of 20 µL where 10 µL of master mix, 0.4 µL of each forward and reverse primer (10 µM), 2 µL of cDNA template, and nucleate-free water were added. Using Applied Biosystems 7500 Real-Time PCR System, amplify was performed using the following cycling conditions: 2 min of initial enzyme activation at 95 °C, follow 40 cycles of 15 s of denaturation, 95 °C, 30 s of annealing/extension at 60 °C, and, as last, a melt-curve analysis of the final product at 65–95 °C in order to confirm product specificity. In this study, primer sequences (5′–3′) were designed from the canine reference mRNA sequences available in GenBank and UniProt for TNF-α, IL-6, IL-8, occludin, claudin-1, ZO-1, GAPDH, and synthesized from Macrogen (Seoul, Republic of Korea). In optimizing the efficiency of RT-qPCR, amplicon sizes were kept below 150 bp.

The primer sets for the study's genes were as follows: TNF-α forward 5′-CAGCCTCTTCTCCTTCCTGAT-3′ along with reverse 5′-GCCAGAGGGCTGATTAGAGA-3′ (132 bp); IL-6 5′-AGACAGCCACTCACCTCTTC-3′ (forward) 5′-CTCAGGGCTGAGATGCCATA-3′ (reverse) (118 bp); IL-8 forward 5′-CTGCTCTCTTGGCAGCCTTC-3′ and reverse 5′-GTGGCAGACCTCGTTTCCAA-3′ (140 bp); occludin forward 5′-CCCCATCTGACTATGTGGAAAGA-3′ and reverse 5′-AAAACCGCTTGTCATTCACTTTG-3′ (125 bp); claudin-1 forward 5′-AAGACGATGAGGTGCAGAAG-3′ and reverse 5′-GTGAAGGCAGGTCTGTATGG-3′ (130 bp); ZO-1 (zonula occludens 1) forward 5′-TGCAGTCTGTGGATGGTTCT-3′ and reverse 5′-CTCTGTCCTCCTGCTTGTTG-3′ (138 bp); and for the control gene (GAPDH) - forward 5′-

GGTGAAGGTCGGAGTGAACG-3′ and reverse 5′-GAGGTCAATGAAGGGGTCGC-3′ (120 bp). The efficiency (90–110%) and specificity (single melt-curve peak and singular band) were confirmed prior to the execution of the experiment. The relative levels of each gene were determined based on the $2^{-}\Delta\Delta Ct$ values for each Sample with GAPDH as the target gene, and the controls accounted for contamination and amplification of extraneous genomic DNA (20,21).

Statistical analysis

Quantitative data across three independent experiments was gathered and analyzed using mean and standard deviation plus or minus. Standard deviation was calculated. Data were analyzed using 9.0 version of GraphPad Prism and SPSS 26.0. To implement an appropriate loss of data, the Shapiro-Wilk test was used. Levene's test checked the overall balance of variance across all of the data. The appropriate procedure of post-hoc analysis was selected. In cases where the normality of the region was not much more relaxed than in the initial analysis, the log of the data was taken prior to tackling the data amelioration. Confidence was instilled regarding the achievement of the overall aim of statistical analysis in the region so that the loss to so be not random, and that it was likely to be used effectively. Evidence relating to the Pearson Value was the variable used. To determine the positive effects of AXOS and LGG. This notated the mechanistic interpretation of the protective effects of AXOS. This also interpreted the Cytokines that were used. This indicated the interpretation of the weak dual hit.

Ethical Approval and Biosafety Issues

In this study, the MDCK cell line, which is immortalized and established, was used. There were no human subjects nor any live experimental animals, which meant that formal human or animal ethics approval was not necessary according to the national regulations. Nevertheless, while using the MDCK cell line, pathogenic P. mirabilis isolates, and BAC, the research protocol was submitted to and obtained approval from the Wasit University, Iraq, Institutional Research and Biosafety Committee (141-Jan-25-2025). All the activities were performed in a BSL–2 laboratory as per the institution’s biosafety regulations, and to reduce the environmental and occupational hazard, all biological and chemical wastes, including BAC-containing media and the bacterial cultures, were disinfected by autoclaving or other suitable chemical disinfectants before disposal.

Results

Impact of AXOS and Lactobacillus rhamnosus GG on MDCK cell viability and cytotoxicity

According to the data from the MTT assay, the exposure of MDCK monolayers to dual-hit injury of P. mirabilis and BAC resulted in a significant reduction in metabolic activity, with viability dropping to about 45–50% of the unexposed control ($p < 0.001$) (Fig. 1).

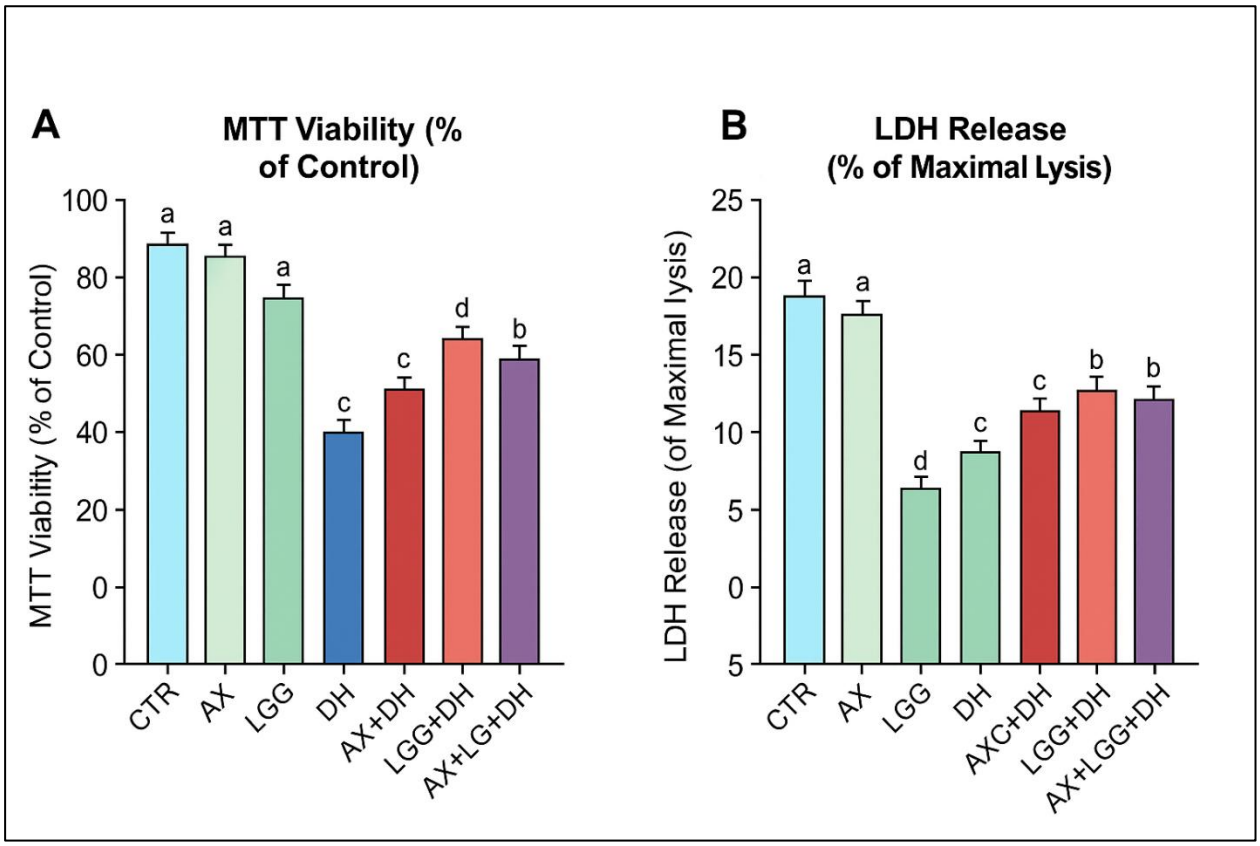

Figure 1. Effect of date-pit AXOS and Lactobacillus rhamnosus GG on MDCK cell viability and LDH release under dual-hit injury with Proteus mirabilis and benzalkonium chloride.

LGG or AXOS alone did not have a significant influence on the loss of viability or did so only to the amount of 95–105% of control ($p > 0.05$). Pre-treatment with AXOS prior to dual-hit exposure was able to partially preserve cell viability at around 65–70% of control ($p < 0.01$ vs dual-hit only), whereas LGG pre-treatment elevated viability to about 70–75% ($p < 0.01$ vs dual-hit only). The combination of AXOS and LGG pre-treatment had the most pronounced protective effect, restoring viability to 85–90% of the unexposed control ($p < 0.001$ vs dual-hit, $p < 0.05$ vs single pre-treatments). LDH release was 2.5–3.0 times the control level and followed an opposite pattern, being quite exhaustive ($p < 0.001$). There was a modest reduction in AXOS or LGG pre-treated groups ($p < 0.01$). The AXOS+LGG group had near control levels of LDH release, signifying that membrane damage was effectively mitigated.

Morphological changes and monolayer integrity in response to treatments

In contrast to affected monolayers, treated MDCK monolayers possessed a continuous cobblestone morphology with tight cell-to-cell contacts and small intercellular junctions, and they presented with no signs of cytotoxic morphology. MDCK monolayers treated with AXOS and LGG, in comparison to AXOS, LGG, and control, also possessed no signs of cytotoxic morphology and similar to AXOS and LGG control groups. Cells treated with AXOS and LGG also distinguished themselves in terms of maintained monolayer integrity, compared to control groups. In comparison to control, cells treated with P. mirabilis and BAC presented with loose cell morphology and absent cell-to-cell contacts, as well as extensive cell detachment causing exposed areas on the underlying culture. Controls, in contrast, presented cohesive monolayer morphology with continuous cell-to-cell contacts. In comparison to control AXOS pretreatment, cells treated with P. mirabilis and BAC presented with reduced intercellular gaps, and LGG pretreatment, while improved in terms of monolayer cohesion, presented with a lower mean cell confluence. Controls lost 48.75 \273 3.11\246 of the monolayer. All these treatments minimized the loss of cell and cell cohesion meant that cells remained adhered to the underlying culture. Monolayers of AXOS + LGG combination pre-treatment also presented confluency, with monolayers presenting

upper cell cohesion that was absent in control. Controls, in contrast to AXOS and LGG, presented with cohesive monolayer morphology with continuous cell-to-cell contacts. When exposed to the P. mirabilis + BAC, cells revealed increased gaps with reduced cell detachment, resulting in exposed areas on the underlying culture. Pretreatment AXOS reduced the loose cell morphology observed with LGG, however intercellular gaps remained although the mean cell morphology was enhanced. All these treatments combined the actions of AXOS and LGG to stabilize and support epithelial monolayer integrity and cohesion under dual-hit stress.

Gene expression modifications caused by pro-inflammatory cytokines, AXOS, and LGG

The combination of P. mirabilis and BAC triggered a substantial remain pro-inflammatory gene expression response. In comparison to the untreated control, TNF-α mRNA was upregulated by about 5.0-fold, and IL-6 and IL-8 by 4.2-fold and 6.0-fold, respectively (all $p < 0.001$). The individually combined factors AXOS or LGG did not substantially change the levels of base cytokines ($p > 0.05$). The cytokine expression levels post dual-hit showed significant reduction to about 2.8, 2.4 and 3.5-fold of control IL-8, IL-6 and TNF-α respectively after dual-hit exposure. Pre-treatment with AXOS ($p < 0.01$ vs dual-hit) and LGG ($p < 0.01$ vs dual-hit) had similar effects. Pre-treatment with AXOS and LGG, in combination, also showed the strongest levels of suppression with respect to IL-8, IL-6 and TNF-α stimulation to 2.0, 1.5, and 1.6-fold of control respectively ($p < 0.001$ vs dual-hit; $p < 0.05$ vs single/AXOS LGG pre-supplement). No-template and no-RT controls confirmed the the mechanism of amplification. All these results testify to the statement that LGG and AXOS, especially synergistically, effectively diminished inflammatory gene response triggered by dual-hit (Fig. 3).

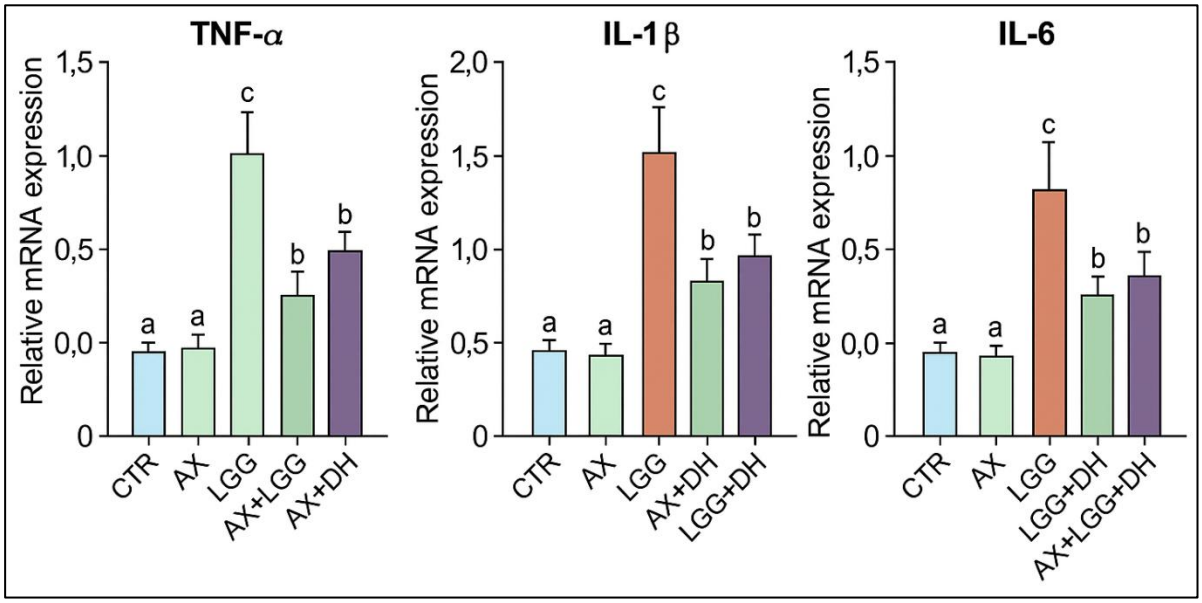

Figure 2. Phase-contrast micrographs of MDCK monolayers showing the protective effects of date-pit AXOS and *Lactobacillus rhamnosus* GG against dual-hit injury induced by *Proteus mirabilis* and benzalkonium chloride.

Impact of interventions on gene expression of tight-junctions (occludin, claudin-1, ZO-1)

In the dual-hit model, there was considerable downregulation of tight-junction genes in MDCK cells, reflecting the disruption of the barrier. Occludin, claudin-1 and ZO-1 mRNA dropped to 0.35, 0.40, and 0.30 in the untreated control, respectively ($p < 0.001$ for all) (Fig 4). Decreases in expression in all three genes suggest that the genes continue to be expressed, however at lower levels. In the presence of AXOS and LGG alone, tight-junction gene expression was baseline (0.9-1.1 fold, $p > 0.05$ vs control) which indicates that there were no adverse effects on the integrity of the junctions.

Prior to the dual-hit challenge, we performed a pre-treatment with AXOS, which was able to

partially recover the transcripts for occludin, claudin-1, and ZO-1, which were 0.65, 0.70, and 0.60 folds to control, respectively ($p < 0.01$ vs dual-hit). Similar LGG pre-treatment restored transcripts from dual-hit to 0.70, 0.75 and 0.65 folds, respectively, to control ($p < 0.01$ vs dual-hit). The combination of AXOS and LGG pre-treatment was able to recover transcripts to the greatest extent, occludin, claudin-1 and ZO-1 were 0.95, 1.0, and 0.90 folds to control and were not significantly different from the untreated group ($p > 0.05$) but were significantly higher than the dual-hit and single pre-treatment groups ($p < 0.05$). This result suggests that AXOS and LGG acted together to recover to a greater extent the expression of the tight-junction preserving genes from the significant drop in occludin, claudin-1, ZO-1 expression that were attributable to P. mirabilis and BAC.

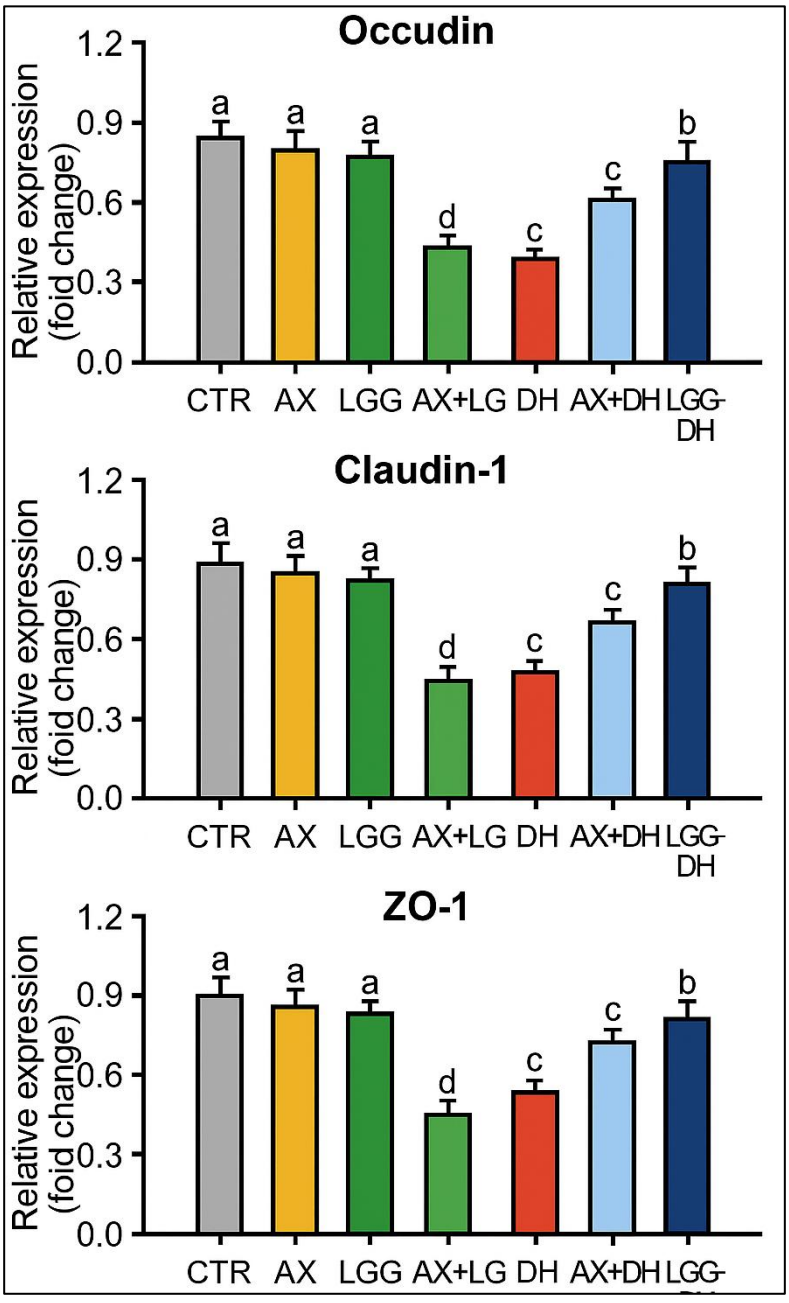

Figure 3. Effect of date-pit AXOS and Lactobacillus rhamnosus GG on the expression of tight-junction genes (occludin, claudin-1, ZO-1) in MDCK cells under dual-hit injury conditions.

Relationship Between Pro-Inflammatory Cytokines and Tight Junction Markers

The analysis of all groups simultaneously demonstrated significant inverse correlations among all

pro-inflammatory cytokines and tight junction genes in all groups simultaneously, which provides evidence of a potential role of inflammation in barrier loss and supports a potential mechanistic connection between inflammation and cell barrier loss (Figure 4, 5). TNF-α expression exhibited significant inverse correlation with occludin ($r = -0.81$, $p < 0.001$), claudin-1 ($r = -0.78$, $p < 0.001$), and ZO-1 ($r = -0.84$, $p < 0.001$). Such inverse patterns were also observed with IL-6 and IL-8, which exhibited significant inverse correlations with tight junction transcripts (r values between -0.70 and -0.82, all $p < 0.01$). In AXOS+LGG pre-treated groups, there were no statistically significant differences in cytokine expression and regression of tight junctions loss, and the overall analyzed data points clustered around the control area in the correlation graphs, which indicates that both treatments resulted in a largely low inflammatory, barrier preserving transcriptional state (Figure 4).

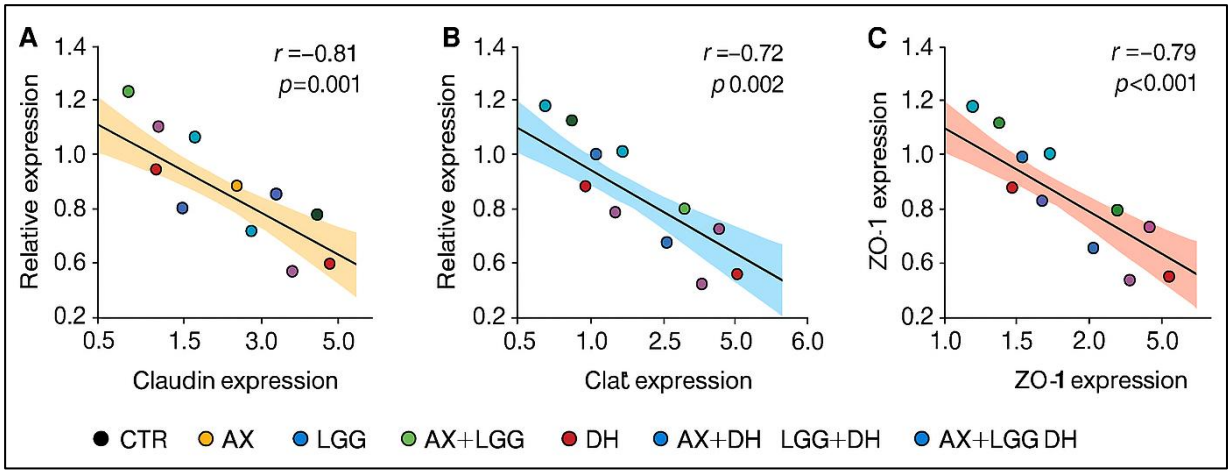

Figure 4. Correlation between pro-inflammatory cytokine expression and tight-junction gene expression in MDCK cells treated with date-pit AXOS and Lactobacillus rhamnosus GG under dual-hit injury.

Discussion

The study indicated that co-treatment with arabinoxylan oligosaccharides (AXOS) and Lactobacillus rhamnosus GG (LGG) along with date pits significantly reduced the dual-hit injury caused by Proteus mirabilis and benzalkonium chloride (BAC) as MDCK kidney epithelial cells demonstrated increased cell viability and tight-junction gene expression, reduced LDH release and maintained tight-junction gene expression. This corresponds with the growing response to date pits, AXOS, and probiotic combinations that bolster the epithelial barrier, and precondition the host to better exploit co-existing microbes. Subhash et al (2024), Leschonski et al (2024), and other scientists demonstrated similar results that arabinoxylan polymer date-seed polysaccharides reduced inflammation, awardingly, and deviated the gut microbial ecosystem to restore dominance of gut eubacteria and augmentation of beneficial microbes by their metabolites, i.e. short-chain fatty acids (SCFAs) and active agents that attenuate oxidative stress. The suppression of triad pro-inflammatory cytokines TNF-α, IL-6, and IL-8 expression and secretion was the primary evidence of the anti-inflammatory potential of AXOS and LGG (Zhang et al. 2024) that had previously described polysaccharides as agents of microbe-epithelial biota and immunomodulatory homeostasis. In keeping with the observations of Orlando et al. (2025) that L. rhamnosus GG defended epithelial cells of the intestine against lipopolysaccharide-induced tight-junction breach by elevating its autophagy, the data presented recovery of expression of mRNA of occludin, claudin-1 and ZO-1 captured by tight junction. The reports read together point to the conclusion that both AXOS and LGG provide synergistic and cytoprotective activity by dampening inflammatory cytokines and fortifying epithelial junctions. These are consistent with theories proposing mechanisms that involve the attenuation of oxidative stress and maintenance of the epithelial barrier.

Additionally, the dual-hit model made use of here recreates the complicated epithelial damage due to pathogen–chemical interactions, simulating the injuries from the environment and from clinical exposures. BAC can be transported via renal organic cation transporters and injure MDCK cell oxidative membranes, as detailed by Vieira et al. (2024). This mechanism BAC explained the steep viability drop witnessed in the dual-hit group. However, highly suggestive of the protective effect of LGG, Torui et al. (2021) demonstrated far less cell death due to the sepsis–induced inflammation in the challenged mice of their control group. Likewise, Gao et al. (2019) postulated that the LGG postbiotics enhance matured defense of the epithelium, thus aiding the restored tight-junction transcription. Nissanka et al. (2025) also supports the anti-virulence aspect of probiotics against P. mirabilis as the mitigation of host damage from P. mirabilis biofilm formation by virulence factors is also detailed. As proposed by Zhang et al. (2024) and Groah et al. (2023), the significant negative correlation between the pro-inflammatory cytokines and the tight-junction genes seen in this study supports the inflammation-damaging loops of barrier that propose control of inflammation and thereby directly keep the epithelial integrity intact.

Conclusion

The results obtained from the dual-hit experimental model show that the combination of lactobacillus rhamnosus GG and arabinoxylan dismissed the cytoprotection and the MDCK cell expectant viability, the pro-inflammatory cytokines, and the tight junction expression levels of the cells challenged with BAC and Proteus mirabilis cytotoxic activity. The combination of AXOS with LGG provides stronger protection against the mdc cytotoxic activity than the single LGG and AXOS additions, giving proof for synergy between the immune defense modulation and epithelial layer protection from BAC and Proteus mirabilis. AXOS and LGG formulations could be used for postbiotic/probiotic alternatives for the protection of infected and disinfected renal epithelium.

Acknowledgment

The authors thank the laboratory staff for technical assistance and support throughout the study.

Conflict of Interest

The authors declare that there are no conflicts of interest related to this work.

Funding

This research was conducted without any external funding support, but it was self-funded by the author.

Author Contributions

All authors participated equally in study design, laboratory work, data analysis, and manuscript preparation.

Data Availability

All data generated or analyzed in this study are available from the corresponding author upon reasonable request.

References

1. Subhash AJ, Bamigbade GB, Tarique M, Al-Ramadi B, Abu-Jdayil B, Kamal-Eldin A, et al. Bioactive properties and gut microbiota modulation by date seed polysaccharides extracted using ultrasound-assisted deep eutectic solvent. Food Chem X. 2024;22:101354. https://doi.org/10.1016/j.fochx.2024.101354
2. Bouaziz F, Noby M, Koubaa M, Rjeibi I, Khlifi S, Ghazala I, et al. Date seeds as a natural source of dietary fibers to improve texture and sensory properties of wheat bread. Foods. 2020;9(6):737. https://doi.org/10.3390/foods9060737

3. Orlando A, Maqoud F, Mallardi D, Drago S, Malerba E, Chimienti G, et al. Lactobacillus rhamnosus GG and Lactobacillus paracasei IMPC2.1 mitigate LPS-induced epithelial barrier dysfunction: a focus on autophagy regulation. Int J Mol Sci. 2025;26(22):11148. https://doi.org/10.3390/ijms262211148

4. Al-Sadi R, Nighot P, Nighot M, Haque M, Rawat M, Ma TY. Lactobacillus acidophilus induces a strain-specific and Toll-like receptor 2-dependent enhancement of intestinal epithelial tight junction barrier and protection against intestinal inflammation. Am J Pathol. 2021;191(5):872-884. https://doi.org/10.1016/j.ajpath.2021.02.003

5. He S, Guo Y, Zhao J, Xu X, Wang N, Liu Q. Ferulic acid ameliorates lipopolysaccharide-induced barrier dysfunction via microRNA-200c-3p-mediated activation of PI3K/AKT pathway in Caco-2 cells. Front Pharmacol. 2020;11:376. https://doi.org/10.3389/fphar.2020.00376

6. Dickson K, Zhou J, Lehmann C. Lower urinary tract inflammation and infection: key microbiological and immunological aspects. J Clin Med. 2024;13(2):315. https://doi.org/10.3390/jcm13020315

7. Yang A, Tian J, Li Y. New insights into Proteus mirabilis virulence in urinary tract infections. Front Cell Infect Microbiol. 2024;14:1465460. https://doi.org/10.3389/fcimb.2024.1465460

8. Prusek A, Sikora B, Skubis-Sikora A, Czekaj P. Assessment of the toxic effect of benzalkonium chloride on human limbal stem cells. Sci Rep. 2025;15(1):12295. https://doi.org/10.1038/s41598-025-96919-2

9. Kanno S, Kakuta M, Tokushige C, Minowa T, Hosoya T, Kurauchi Y, et al. Plasma membrane damage triggered by benzalkonium chloride and cetylpyridinium chloride induces G0/G1 cell cycle arrest via Cdc6 reduction in human lung epithelial cells. J Toxicol Sci. 2023;48(2):75-86. https://doi.org/10.2131/jts.48.75

10. Lou Q, Xu M, Misra SL, Mugisho OO, Rupenthal ID, Craig JP. Suppression of NLRP3/caspase-1/GSDMD-mediated corneal epithelium pyroptosis using melatonin-loaded liposomes to inhibit benzalkonium chloride-induced dry eye disease. Int J Nanomed. 2023;18:2447-2463. https://doi.org/10.2147/IJN.S403337

11. Subhash AJ, Bamigbade GB, Tarique M, Al-Ramadi B, Abu-Jdayil B, Kamal-Eldin A, et al. Bioactive properties and gut microbiota modulation by date seed polysaccharides extracted using ultrasound-assisted deep eutectic solvent. Food Chem X. 2024;22:101354. https://doi.org/10.1016/j.fochx.2024.101354

12. Leschonski KP, Mortensen MS, Hansen LBS, Krogh KBRM, Kabel MA, Laursen MF. Structure-dependent stimulation of gut bacteria by arabinoxylo-oligosaccharides (AXOS): A review. Gut Microbes. 2024;16(1):2430419. https://doi.org/10.1080/19490976.2024.2430419

13. Zhang W, Zhang Y, Zhao Y, Li L, Zhang Z, Hettinga K, Yang H, Deng J. Dietary polysaccharides: Emerging prebiotics and modulators of gut microbiota in health and disease. Nutrients. 2024;16(23):4122. https://doi.org/10.3390/nu16234122

14. Orlando A, Maqoud F, Mallardi D, Drago S, Malerba E, Chimienti G, Russo F. Lactobacillus rhamnosus GG and Lactobacillus paracasei IMPC2.1 mitigate LPS-induced epithelial barrier dysfunction: a focus on autophagy regulation. Int J Mol Sci. 2025;26(22):11148. https://doi.org/10.3390/ijms262211148

15. Chusak C, Mayuree O, and colleagues. Enhancing viability of Lactobacillus rhamnosus GG and total polyphenol content in fermented black goji berry beverage through calcium-alginate encapsulation with hydrocolloids. Foods. 2025;14(3):518. https://doi.org/10.3390/foods14030518

16. Vieira LS, Hallinger DR, Eytan O, Kato M, Higgins JW, Hillgren KM. Interaction and transport of benzalkonium chlorides by human organic cation transporter 2 in Madin-Darby canine kidney II cells. Drug Metab Dispos. 2024;52(4):351-360. https://doi.org/10.1124/dmd.123.001625

17. Groah SL, Reddy A, Gormley BG, et al. Intravesical Lactobacillus rhamnosus GG alters urobiome composition: implications for urinary tract infection prevention and management. Urology. 2023;174:58-65.

18. Tsui KC, Yen TL, Huang CJ, Hong KJ. Lactobacillus rhamnosus GG as dietary supplement improved survival from lipopolysaccharides-induced sepsis in mice. Food Sci Nutr. 2021;9:6786-6793. https://doi.org/10.1002/fsn3.2630

19. Gao J, Guo L, Gao Q, Liu X, Yan M, Yin J. A novel postbiotic from Lactobacillus rhamnosus GG accelerates the maturation of neonatal intestinal defense. Front Pediatr. 2019;7:103. https://doi.org/10.3389/fmicb.2019.00477

20. Nissanka A, Katongole P, Li F, Li X. Decoding Proteus mirabilis biofilm formation and virulence in urinary tract infections. Front Cell Infect Microbiol. 2025;15:1465460